

See discussions, stats, and author profiles for this publication at: <https://www.researchgate.net/publication/241698421>

Creation of Self-Organized Complex Meso Patterns in Sol–Gel Thin Films by Confined Capillary Dynamics

ARTICLE in INDUSTRIAL & ENGINEERING CHEMISTRY RESEARCH · JUNE 2012

Impact Factor: 2.59 · DOI: 10.1021/ie300012m

CITATIONS

4

READS

59

7 AUTHORS, INCLUDING:



Devika Sil

Temple University

11 PUBLICATIONS 48 CITATIONS

[SEE PROFILE](#)



Sunirmal Jana

CSIR-Central Glass and Ceramics Research Ins...

36 PUBLICATIONS 275 CITATIONS

[SEE PROFILE](#)



Rabibrata Mukherjee

IIT Kharagpur

35 PUBLICATIONS 422 CITATIONS

[SEE PROFILE](#)

Creation of Self-Organized Complex Meso Patterns in Sol–Gel Thin Films by Confined Capillary Dynamics

Rimlee Deb Roy,[†] Devika Sil,^{‡,§,⊥} Sunirmal Jana,[‡] Nandini Bhandaru,^{||} Shyamal Kumar Bhadra,[†] Prasanta Kumar Biswas,^{*,‡} and Rabibrata Mukherjee^{*,§,||}

[†]Fibre Optics & Photonics Division, [‡]Sol–Gel Division, and [§]Analytical Facility Division, CSIR–Central Glass & Ceramic Research Institute, 196 Raja S. C. Mullick Road, Jadavpur, Kolkata 700 032, India

^{||}Department of Chemical Engineering, Indian Institute of Technology Kharagpur, West Bengal 721 302, India

ABSTRACT: We report a simple and facile technique for creating complex mesoscale patterns with two-dimensional (2-D) orders on the surface of a sol–gel derived silica thin films using a combination of a topographically patterned stamp and a substrate, each having a one-dimensional (1-D) grating structure (stripes). The self-organized pattern formation results as a consequence of capillary flow of the sol film in liquid state under a confining stamp. The key novel aspect of the work lies in using a topographically patterned substrate, dip coating on which results in a film with an undulating top surface. When a grating stamp is brought in conformal contact with such a film in a manner so that the direction of the stamp stripes are at right angles to the direction of the undulations on the film surface, a periodically ordered spatial variation in the extent of contact between the film and the stamp results. Subsequent capillary flow of the liquid sol along the stamp walls occurs only at the locations where the stamp surface and the film are in direct contact, resulting in an array of pillars with 2-D order. We further show that the morphology of the final patterns can be tailored by varying various parameters such as the initial film thickness, wettability of the stamp, and periodicity of the substrate. We further discuss the gradual oxidation of the sol film with progressive thermal annealing and the associated shrinkage of the structures in terms of pattern dimensions. Generation of meso patterns with 2-D order on an inorganic sol–gel film surface using a stamp and a substrate, each having strictly 1-D features, is the key novel aspect of the work, as it is a rare example when patterns other than a mere negative replica of a stamp are created on a sol–gel thin film by any soft lithography technique.

1. INTRODUCTION

Topographically patterned films and surfaces with mesoscale patterns find extensive application in various areas such as microelectronics,¹ nanobiotechnology,² super hydrophobic and self-cleaning surfaces,³ structural color,⁴ patterned adhesives,⁵ and microfluidics.⁶ While photolithography remains the preferred technique for conventional microelectronics,¹ various soft lithography methods,^{7,8} such as capillary force lithography (CFL),^{9,10} micromolding in capillaries (MIMIC),¹¹ replica molding (REM),¹² nanotransfer printing,¹³ and their numerous derivatives along with nanoimprint lithography (NIL),^{14,15} are widely used for fabricating defect-free, large area, high fidelity patterns in soft materials, particularly in polymers and gels.^{7,16} Each of these techniques is capable of producing a perfect negative replica of the stamp pattern,^{7–15} and thus the success of any soft lithography method depends to a large extent on the availability of an appropriate stamp. While methods like NIL directly use a lithographically fabricated rigid mold,^{14,15} most soft lithography methods rely on using a cross-linked polydimethylsiloxane (PDMS) stamp, which is first fabricated by molding the elastomer (PDMS) against a lithographically fabricated master.^{7–13} Techniques such as focused ion beam (FIB) writing, electron beam lithography (EBL), and photolithography are generally used for fabricating the original master or mold, the fabrication cost of which enhances exponentially with increased complexity of its design.¹⁷ Thus, right from the beginning of soft lithography research, there have been attempts to create complex two-dimensional (2-D) patterns

using simple stamps.¹⁸ While some recently developed methods such as elastic contact lithography (ECL) have the potential of generating ordered 2-D patterns with a simple grating stamp in one step,^{19,20} in most cases multiple imprinting of a softened film with a one-dimensional (1-D) grating stamp is adopted for creating complex patterns, with a simple grating stamp.^{21–24} In this approach, the film is initially imprinted with the first stamp to obtain a negative replica and subsequently, the second stamp is placed on the prepatterned film with a rotated line of orientation with respect to the direction of the patterns already existing on the film surface, resulting in ordered 2-D structures such as an array of pillars or holes.^{21–24,45} An effective sequential double imprint is possible only when the primary structures do not relax completely while the secondary patterns form. Simultaneously, it is also essential that the primary structures remain in a softened state to facilitate morphological self-organization during the second imprinting. Therefore, the success of multiple imprinting based approaches, which have mostly been reported for polymer thin films,^{21–24} depends largely on the appropriate rheological condition during imprinting the film.

Soft lithography as a generic technique is no longer limited to polymeric thin films and has been extensively used for sol–gel

Received: January 2, 2012

Revised: June 15, 2012

Accepted: June 20, 2012

Published: June 20, 2012



Table 1. Details of the Patterned Stamps and Substrates Used

Stamp/Substrate Type	Material	Periodicity (λ_p)	Line width (L_p)	Stripe height (h_p)	Schematic Representation	
Type 1 Substrate	Polycarbonate	1.5 μm	750 nm	120 nm		
Type 1 Stamp	PDMS					
Type 2 Substrate	Polycarbonate	800 nm	400 nm	70 nm		
Type 2 Stamp	PDMS					

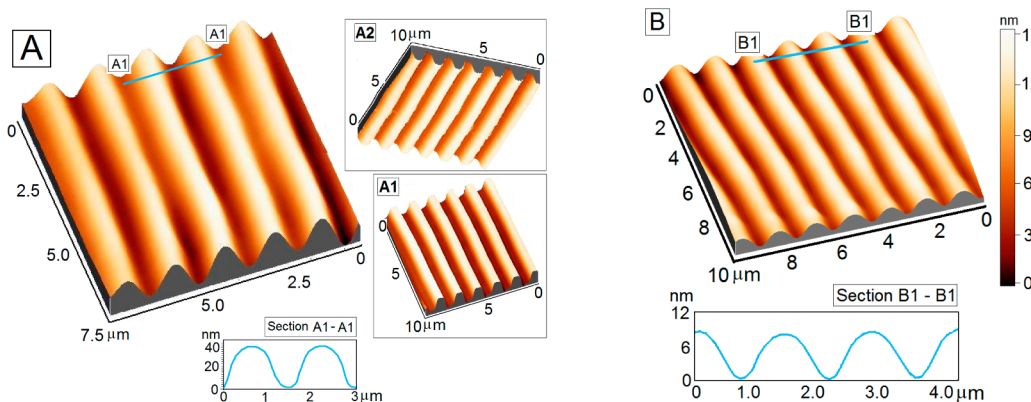


Figure 1. (A) Morphology of an as-coated silica sol film on a type 1 polycarbonate substrate. Insets A1 and A2 show the morphologies of a type 1 cross-linked PDMS stamp and a type 1 PC substrate, respectively. The film $h_E \sim 440$ nm, and the cross-sectional line scan show $A_F \sim 33$ nm. (B) Morphology of an as-coated silica sol film with $h_E \sim 690$ on a type 1 PC Substrate. The cross-sectional line scan shows $A_F \sim 8$ nm.

precursors for patterning inorganic thin films.^{25–46} For example, MIMIC has been used for patterning ionic salts and glasses.^{25,28,29} Trau et al. used a combination of micromolding and self-assembly to obtain micropatterned silica films with a high degree of orientation order.²⁷ Mesoscale patterns on various types of inorganic materials and systems such as silica,²⁸ titania,⁴¹ mixed sols (silica–titania),^{40,41} phosphors,³⁵ PbTiO₃, lead zirconate titanate (PZT, Pb(ZrTi)O₃),^{30,37,45} strontium niobate (Sr₂Nb₂O₇),³⁰ borosilicon carbonitride (SiBNC),³⁴ and organic–inorganic hybrid materials,³⁹ with resolutions down to as low as ~ 200 nm, have been achieved,⁴⁵ by adopting various soft lithography methods.

Careful scrutiny of the published literature reveals that, except one recent paper,⁴⁶ all the papers on soft lithographic patterning of sol–gel thin films are limited to the formation of a negative replica of the stamp geometry only. Thus, the flexibility that the scientific community has been able to harvest in terms of generating complex topographic structures with simple 1-D stamps in polymers has remained elusive in inorganic systems. This is due to the fact that, unlike a polymer, a sol–gel film cannot be softened by thermal annealing or solvent vapor exposure, which is essential for sequential multiple imprinting. In contrast, thermal annealing of a sol–gel film results in a sol to gel transformation, with further stiffening of the material. Sequential imprinting has only recently been possible in films of inorganically cross-linked sol–gel (ICSG) materials, which is a special class of material that has low initial viscosity and extreme thermal, chemical, and mechanical stabilities.⁴⁶ However, multiple imprinting based complex patterning has never been implemented in classical and simple sol–gel systems.

In this article we demonstrate that complex 2-D patterns in a sol–gel thin film can be generated with two gratings, using one of them as the stamp and the other one as a topographically patterned substrate. Direct coating of a thin film on a topographically patterned substrate results in a film with an undulating top surface. The topographically patterned stamp is placed on the film surface in such a manner that the direction of stamp stripes remain perpendicular to that of the surface undulations. This results in a periodic spatial variation in the extent of contact between the film and the stamp. The liquid sol undergoes capillary flow at locations where the film and the stamp are in conformal contact, resulting in self-organized mesoscale patterns with 2-D lateral ordering. The use of a stamp and a substrate, both having simple 1-D grating structures, to generate complex patterns on a sol–gel thin film is the key novelty of this work, which is a rare example where patterns other than a mere negative replica of the stamp have been obtained on a thin sol–gel film.

2. EXPERIMENTAL DETAILS

2.1. Substrate. As low-cost readily available substrates with grating geometry, the patterned polycarbonate parts of commercially available optical data storage disks (CD and DVD) have been used.²⁴ In these disks, a single spiral track is drilled on the polycarbonate (PC) disk. As the radius of the disk is much larger compared to the gap between two adjacent turns of the spiral, under the field of view of any microscope the pattern on a CD/DVD disk appears as a grating. The line width (L_p), stripe periodicity (λ_p), and feature height (h_p) of the substrates used can be found in Table 1. Typically, 25 mm \times 15 mm rectangular pieces cut from the disks were used as substrates in our experiments. The protective aluminum foils of

the disks were peeled off to reveal the clean, patterned substrate just before coating. The morphology of a type 1 PC substrate can be seen in inset A1 of Figure 1A.

For the thermal annealing experiments which were performed for understanding the sol to gel transformation and to study the shrinking effects (discussed later), the PC disks could not be used as they melted at high temperature. Therefore, quartz pieces (both sides polished) were used as substrates for these experiments only.

2.2. Stamp Fabrication. The cross-linked PDMS stamps were fabricated by replica molding against the patterned polycarbonate masters obtained from CD/DVDs (identical to the ones used as substrates), with a 10:1 (wt/wt) mixture of part A (elastomer) and part B (cross-linker) of Sylgard 184 (Dow Corning, U.S.A.). The prepolymer solution, after degassing, was poured onto the mold and was thermally annealed at 130 °C for 12 h for complete cross-linking, after which the stamp was manually peeled off. The dimensional details of the various types of stamps used can be found in Table 1. The morphology of a type 1 cross-linked PDMS stamp can be seen in inset A2 of Figure 1A.

Cross-linked Sylgard 184 is inherently hydrophobic as it exhibits a water contact angle of ~110° (measured by a contact angle goniometer, Rame Hart, USA, Model 290). It also exhibits a finite contact angle (~35°) with 1-propanol and 2-butanol, which are the key solvents present in the silica sol film. As the pattern replication process is based on capillary driven flow, it is essential that the stamp material is preferentially wetted by the sol film. The stamps were made completely wettable by exposing the patterned surface of the stamps to UV ozone exposure for 30 min in a UV ozone chamber (locally fabricated), just prior to imprinting the films. UV irradiation at 185 nm wavelength produces ozone from atmospheric oxygen, which subsequently gets dissociated to atomic oxygen at 254 nm irradiation. The atomic oxygen reacts with the siloxane group of the PDMS, forming a stiff surface layer consisting of oxides of silicon. This layer enhances the wettability of the Sylgard stamp surface.^{20,24} To show the effect of stamp wettability on the final morphology of the patterns, we also performed some experiments in which the stamps were not exposed to UV ozone and therefore remained partially wettable by the solvents.

2.3. Preparation of Silica Sol. The silica sol was prepared by mixing tetraethoxysilane ($\text{Si}(\text{OC}_2\text{H}_5)_4$, TEOS, 98% purity, Fluka Chemika) and 1-propanol (1-C₃H₇OH, ≥99% purity, E. Merck India Ltd. (EMIL)) under stirring followed by subsequent gradual addition of water. Concentrated HCl (GR grade, EMIL) was used as a catalyst in the reaction. After stirring for 1.5 h, the sol was diluted with a definite amount of 2-butanol (2-C₄H₉OH, ≥99% purity, EMIL). The volume ratio of $\text{Si}(\text{OC}_2\text{H}_5)_4:1\text{-C}_3\text{H}_7\text{OH}:2\text{-C}_4\text{H}_9\text{OH}:\text{H}_2\text{O}:\text{HCl}$ was maintained at 1:2.24:1.66:0.22:0.004.⁴⁶ Double distilled water was used as the hydrolyzing agent for the preparation of sols. The silica sol was aged for 20 h before coating.

2.4. Film Coating. The films were dip coated (Chemate 200 Dip Coater) on the patterned polycarbonate substrates using a silica sol with 16% concentration, at withdrawal speeds varying between 6 and 24 cm/min. Films with other sol concentration (4 and 12%) were also cast in some experiments, particularly to investigate the effect of shrinkage during thermal annealing. As already mentioned, dip coating on a grating substrate results in a film with an undulating top surface with periodic spatial variations in film thickness, which are in phase with the

substrate patterns.⁴⁷ Generally, the film is thicker over the valleys and thinner over the stripes of the grating substrate.⁴⁸ This is attributed to accumulation of material within the grooves during the coating process. Due to the periodic spatial variation of the film thickness, there is no simple way to uniquely identify the film thickness of a film coated on a patterned substrate. Consequently, an equivalent film thickness (h_E) is used, which corresponds to the thickness of a film coated on a flat substrate under identical conditions. In our experiments, we have used films with h_E varying between 300 and ~700 nm, which were obtained by varying the withdrawal speed from 6 to 24 cm/min.⁴⁹ The corresponding amplitude of the surface undulations (A_F) varied from ~36 to ~8 nm on a type 1 PC substrate. Figure 1A shows the morphology of a film coated at 12 cm/min on a type 1 PC substrate, where h_E and A_F are ~440 nm and ~33 nm, respectively. Figure 1B shows the morphology of a film coated on an identical substrate with h_E ~690 nm, obtained at a withdrawal speed of 24 cm/min. It can be clearly seen in the figure that A_F has significantly reduced to ~8 nm.

It was further verified that the orientation of the substrate stripes during dipping (whether the stripes are oriented in the direction of dipping or perpendicular to it) has no significant contribution on the film morphology. It was also checked that the PC substrates were not affected/damaged in any way by the solvents during the dip-coating process.

The thickness and refractive index of the films coated on flat surfaces were measured using an ellipsometer equipped with a He–Ne red laser of wavelength 632.8 nm (Gaertner Auto-Gain Ellipsometer, L-116 B).

At this point we would like to emphasize that dip coating of a sol–gel film generally results in films of higher thickness, typically in the range of a few micrometers. However, here we have been able to obtain films with submicrometer thicknesses. The nonwettability of the PC substrates is primarily responsible for obtaining thinner films.⁵⁰ For example, a 640 nm thick film was obtained on a flat silicon wafer substrate at a withdrawal speed of 12 cm/s. In contrast, on a flat PC substrate the film thickness was found to be ~440 nm under identical coating conditions. The substrate nonwettability results in additional drainage of the liquid during the dipping process, resulting in thinner films on a PC substrate.

2.5. Film Patterning. For patterning the films, the Sylgard stamps were gently brought in conformal contact with the surface of the as-coated films in such a manner that the stamp stripes were oriented at right angles to the directions of the undulations on the film surface. No external pressure was applied on the stamp for embossing. This implies that the pattern formation is not due to a viscoplastic deformation of the sol film under applied external load but is purely due to capillary driven flow of the liquid film along the contours of the stamp in contact with the film. In order to sustain the capillary dynamics, it was essential that the film remained in a liquid (low viscosity) state for the entire duration of pattern replication. This was ensured by reducing the solvent evaporation rate from the film by placing it, along with a stamp, in a chamber presaturated with solvent vapor. The film–stamp assembly was taken out of the solvent chamber after a contact time of ~15 min. The samples were subsequently removed from the solvent chamber and were kept under vacuum inside desiccators, along with the stamp, for ~12 h. Subsequently, the stamp was manually peeled off. The steps associated with pattern replication are schematically shown in

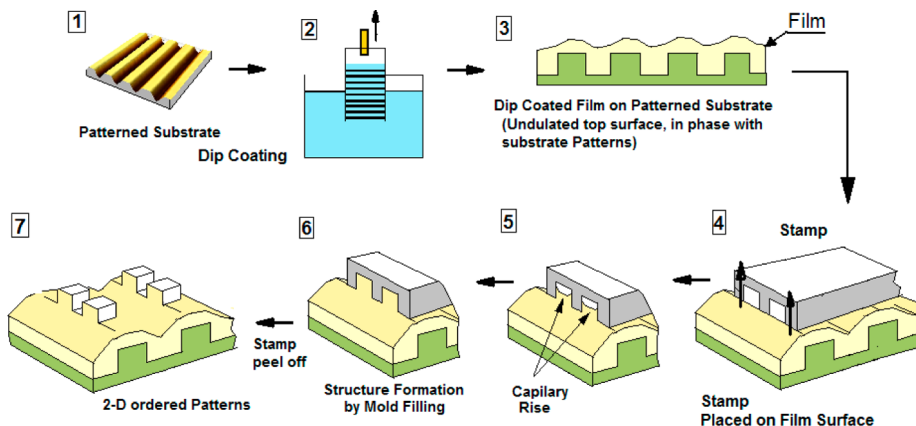


Figure 2. Schematic representation of the method, highlighting the key steps.

Figure 2. The morphology of the patterned films was investigated using an atomic force microscope (AFM; Nanonics) with a silicon cantilever under intermittent contact imaging mode.

2.6. Postpatterning Thermal Annealing. One of the key differences of patterning between an inorganic thin film and a polymer film is the postpatterning thermal processing step to generate the oxide phase from the gel films. In order to achieve this, the samples after patterning were subjected to thermal annealing in oxygen atmosphere, in a closed furnace. The temperature was gradually raised from 50 to 400 °C at a temperature rise rate of 1 °C in 5 min. The samples were further soaked at 400 °C for 4 h before being withdrawn from the furnace. To understand the progressive phase transformation as well as shrinkage of the structures with temperature, some samples were taken out of the furnace at certain intermediate temperatures. Fourier transform infrared (FTIR) spectra as well as AFM scans were performed on all samples which were taken out of the oven at different temperatures. The details about the formation of the oxide phase due to high temperature annealing can be found elsewhere.⁴¹

3. RESULTS AND DISCUSSION

3.1. Patterning of Sol–Gel Films Coated on Topographically Patterned Substrates. The key novelty of the work reported in this article is the possible fabrication of ordered 2-D structures on a thin sol–gel film, using a topographically patterned stamp and a substrate, both having 1-D grating structures. Figure 3 presents the distinct morphologies obtained by using substrates and stamps with different geometries and stamp wettabilities. It is further shown that the morphology of the patterns depends on the initial h_E . For patterning, the grating stamp is first placed in conformal contact with the film coated on the patterned substrate in such a fashion that the stamp stripes are oriented at right angles to the direction of the film surface undulations (shown schematically in Figure 2, frame 4). This results in a periodic spatial variation in the extent of contact between the undulating film surface and the stamp (inset A3, Figure 3A). Due to the capillary effect, the liquid sol film starts climbing along the side walls of the stamp at locations where the film surface is in direct contact with the stamp (inset A4, Figure 3A), resulting in the formation of isolated 2-D pillars. In case of a completely wettable stamp, the rise of the liquid continues until the advancing meniscus reaches the base of the stamp valleys.

Figure 3A shows the pattern morphology when a completely wettable UV exposed type 1 PDMS stamp is used with a film having $h_E \sim 440$ nm, coated on a type 1 PC substrate. The corresponding A_F is ~ 33 nm (Figure 1A). Inset A1 of Figure 3A shows the morphology of the as-coated film, and inset A2 shows the orientation of the stamp with respect to the surface undulations on the coated film. The height of the pillars is ~ 120 nm, which corresponds to the depth of a type 1 stamp. The roof dimension of each pillar is ~ 750 nm² and the periodicities of the pillars in both X and Y directions are $1.5\ \mu\text{m}$, which are entirely governed by the periodicities of the stamp and the substrate used (both type 1). The pillar edges are rather sharp, emphasizing that the features are of high fidelity. Figure 3B shows similar structures with smaller lateral dimensions and periodicities, which were obtained when a completely wettable type 2 stamp and a type 2 PC substrate were used. The h_E and A_F were 370 nm and 29 nm, respectively. The resultant patterns show pillar periodicity of 800 nm in both X and Y directions. Careful observation reveals that the patterns in Figure 3B have archlike tops, in contrast to a flat roof shown in Figure 3A. This is attributed to the geometry of the DVD disks, which themselves have an curved cross section, rather than having square grooves like a CD.²⁴

Figure 3C shows that an array of rectangular pillars can be obtained by using a stamp and a substrate with different periodicities. In this particular case, a type 1 PC substrate and a completely wettable type 2 PDMS stamp were used. The effective film thickness was maintained at 440 nm, with $A_F \sim 33$ nm. The resulting pillars have a height of ~ 70 nm in one direction (which corresponds to the height of a type 2 stamp) and a height of ~ 100 nm in the other direction, which corresponds to the summation of the feature height of the stamp (70 nm) and $A_F \sim 33$ nm. The periodicities of the pillars are $1.5\ \mu\text{m}$ and 800 nm along the two lateral directions.

Figure 3D shows the influence of the initial effective film thickness (h_E) on the final pattern morphology. This figure also emphasizes that the success of the proposed technique depends to a large extent on the amplitude of the film surface undulations. In Figure 3D, a film with $h_E \sim 690$ nm was coated on a type 1 PC substrate. The corresponding A_F was ~ 8 nm only. A low value of A_F results in a weak contrast in the extent of spatial contact along each stamp stripe. Consequently, when the capillary rise starts along the stamp wall, the liquid over the areas which are not in direct contact also starts climbing along the stamp walls, as shown schematically in the inset of Figure 3D. This results in the formation of almost a

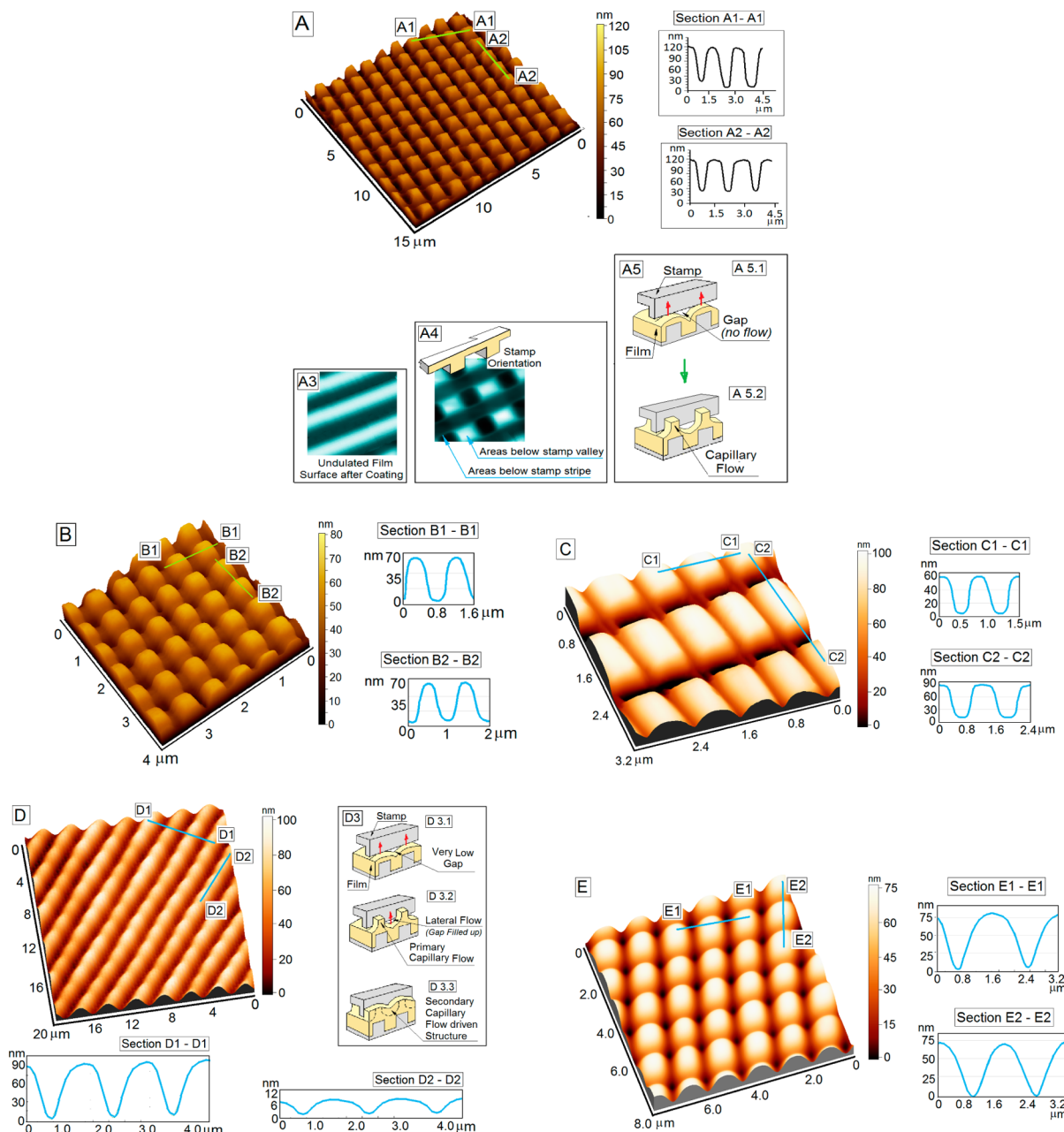


Figure 3. Final morphology of the complex 2-D patterns obtained under various conditions. (A) Array of square pillars obtained on a silica film with $h_E = 440$ nm and $A_F = 31$ nm, coated on a type 1 PC substrate, imprinted with a type 1 completely wettable (CW) cross-linked PDMS stamp. Inset A3 shows the morphology of the as-cast film on the patterned substrate, and inset A4 shows the orientation of the stamp. (B) Array of square pillars obtained on a silica film with $h_E = 370$ nm and $A_F = 29$ nm, coated on a type 2 PC substrate, imprinted with a type 2 CW cross-linked PDMS stamp. (C) Array of rectangular pillars using a type 1 PC substrate and a CW type 2 stamp. (D) Loss of 2-D ordering in a film having $h_E = 690$ nm and $A_F = 8$ nm, coated on a type 1 substrate and imprinted with a CW type 1 PDMS stamp. (E) Loss of fidelity of final patterns when a partially wettable stamp is used. For (C) and (E), h_E and A_F are identical to those used in (A).

negative replica of the stamp pattern on the film surface. As can be seen in Figure 3D, the pattern morphology is similar to a grating and is in complete contrast to an array of square pillars obtained in cases where A_F is significantly higher. On the basis of this observation, it can be concluded that the quality of the 2-D complex patterns gradually deteriorate with progressive reduction of A_F , vis-à-vis gradual increase in h_E .

The influence of the stamp wettability on the morphology of the final patterns is shown in Figure 3E. Here, experimental conditions were kept identical to those used in the case of Figure 3A, except that the stamp used was not UV treated and

therefore was not completely wettable. It can be seen from Figure 3E that the lack of complete wettability of the stamp affects the final morphology of the square pillars in the form of loss of fidelity. The lack of complete wetting of the stamp by the solvents present in the sol film prevents filling of the entire space under the stamp valleys by the rising meniscus, and consequently, the geometry of the pillar roofs does not reflect complete mold filling as it is governed by the finite intrinsic contact angle of the sol film with the partially wettable stamp. As can be seen from the cross-sectional analysis in Figure 3E, the maximum height of the pillars is close to ~80 nm, in

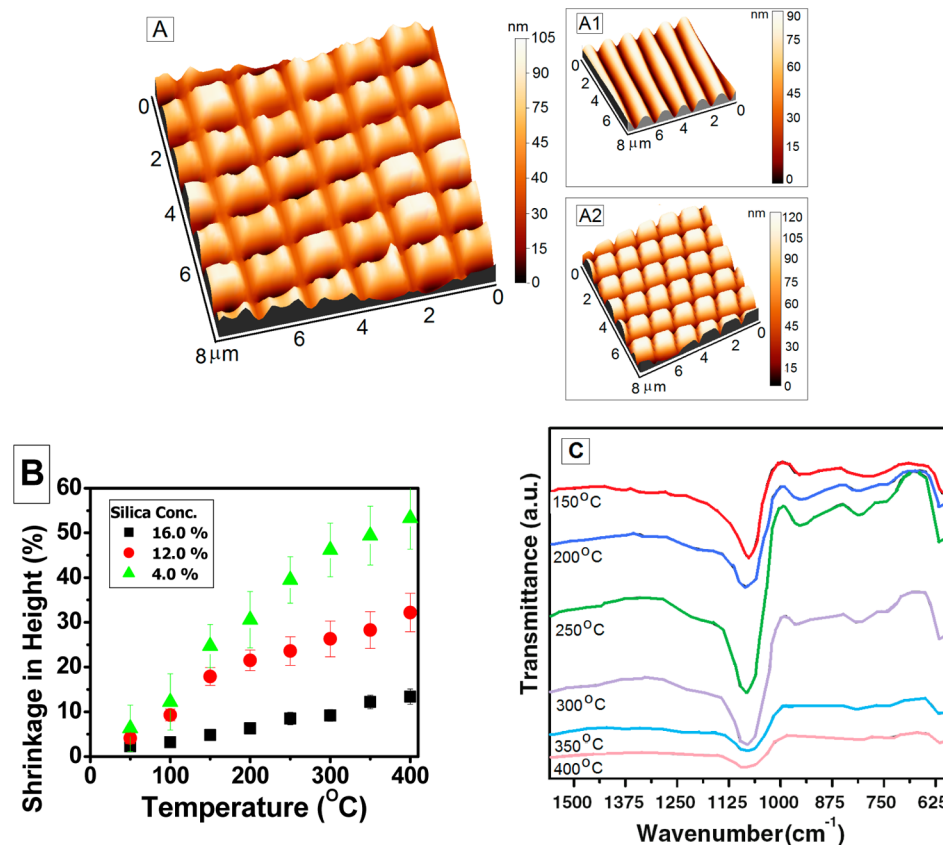


Figure 4. (A) Morphology of the patterns after thermal annealing at 400 °C. Inset A1 shows the morphology of the grating patterned silica substrate on quartz, and inset A2 shows the morphology of the patterns before annealing. (B) Progressive shrinkage in pattern dimension with gradual increase of annealing temperature, for different solute concentrations. (C) FTIR spectra of a 2-D patterned 16% silica sol film with progressive increase in temperature during annealing.

contrast to a pillar height of ~110 nm under identical experimental conditions with a completely wettable stamp, shown in Figure 3A.

Finally, we would like to add that the pattern morphologies obtained are extremely repeatable. At least five experiments were performed for each experimental condition, to verify the repeatability of the process.

3.2. Shrinkage during Thermal Annealing. As already mentioned, it is necessary that the patterned sol–gel films are subjected to a post patterning thermal annealing step, when the sol film condenses to the desired oxide phase as a result of thermochemical decomposition of the alkoxide groups. This stage is also associated with significant shrinkage in terms of the feature dimension of the patterns. In our experiments, the patterned films were annealed up to 400 °C. The effect of structural and chemical changes on a silica sol is extremely well investigated and reported by several groups.⁵¹ The weight loss and chemical effects with temperature due to removal of adsorbed water, Si–OH, and organics in silica gels are studied by thermogravimetric analysis (TGA)/differential thermal analysis (DTA). Generally, the loss of adsorbed water and liquids of low boiling points (such as ethanol, 2-butanol, and 1-propanol) from the gel structure may take place below 300 °C, whereas loss of Si–OH and organics may be found above 300 °C. However, these analyses require bulk samples and cannot be performed with the patterned thin films. Therefore, in this article we do not report any DTA/TGA studies as the results cannot be directly correlated to the changes in the morphology of the film during annealing, which has been studied using

AFM. Details about the progressive oxidation with thermal annealing can be found elsewhere.⁴¹ However, the key findings along with the influence of thermal annealing on shrinkage of the pattern morphology of the complex 2-D structures is described here. As already mentioned, a silica (quartz) substrate was used for these experiments, which was first coated with a silica sol film and subsequently imprinted with a type 1 fully wettable PDMS stamp to generate a grating pattern. Subsequently, it was annealed to 400 °C first to obtain a pure silica structure.⁴¹ The morphology of the silica grating is shown in inset A1 of Figure 4A. The sol film was coated on this patterned silica substrate ($h_E \sim 450$ nm, $A_F \sim 28$ nm) and subsequently imprinted with a completely wettable type 1 PDMS stamp. The morphology of the final 2-D patterns generated this way is shown as inset A2 of Figure 4A. It can be noticed that the morphology significantly resembles the patterns shown in Figure 3A. The 2-D patterned film was subsequently annealed in an air oven, and the post thermal annealing final pattern morphology is shown in Figure 4A. It can be seen from the cross-sectional analysis that the height of the pillars have reduced to ~104 nm from a height of ~120 nm before annealing, suggesting that there is a shrinkage of ~13% due to thermal annealing. However, we observed no change in the lateral periodicity of the patterns. We would like to highlight that, as a patterned silica grating has been used as substrate, the resultant structure after thermal annealing is a complex pattern in pure silica.

To understand the extent of shrinkage as a function of annealing temperature, samples were withdrawn from the oven

after a rise of every 50 °C and scanned with an AFM. FTIR analysis of each partially annealed sample was also performed, which is shown in Figure 4B. It can be seen from the broadening of the spectra in the region 1300–1000 cm⁻¹ that the silica gel film gradually gets transformed to a pure oxide with the decomposition of the organics, with increase in temperature. The broadening of the peak is attributed to an increase in the Si—O—Si network due to progressive oxidation within the film. Further increase of the annealing temperature enhanced the broadening due to cross-linking of the Si—O—Si network which may indicate the film densification. It is also observed that the FTIR vibrations responsible for organics started to diminish beyond a temperature of 300 °C.

The gradual shrinkage of the features with increase in temperature is shown in Figure 4C, where it can be seen that the extent of shrinkage also depends on the initial silica concentration in the sol film. While the final shrinkage is restricted to only about 13% for a film with 16% sol concentration, it is observed to be as high as ~56% for a film with 4% initial silica concentration. The shrinkage is also partially affected by the rate of heating during thermal annealing. However, a detailed discussion on this theme is beyond the scope of this article.

4. CONCLUSIONS

In conclusion, we have presented an extremely simple, easy to implement technique by which complex meso patterns with 2-D order can be created on the surface of a sol–gel derived silica film by using a topographically patterned stamp and a substrate, each having 1-D grating patterns. The patterns shown in Figure 3 could have easily been obtained using expensive custom-made stamps with 2-D patterns,^{28,40,43} or by complex electron beam writing.⁵² However, the proposed method shows that similar patterns with complex geometry can be created without using such costly stamps or techniques, thereby making the approach extremely cost-effective and ideally suited for bulk nano applications. Further, the possible use of CD/DVD disk components for fabrication of stamps and substrates demonstrates that the method can be implemented by all, including nonexperts in soft lithography, without any major tools and instruments. This apparently simple method, however, is one of the first instances where patterns other than a mere negative replica of a stamp have been obtained on a sol–gel derived thin film by any soft lithography technique. Further, though the experiments reported in this article are performed with silica films, the process is generic and can be implemented with films of other materials as well, including polymers. The “do it yourself” type technique does not require any major tools and instruments, and is ideally suited for the fabrication of low-cost large area inorganic templates for various bulk nano applications. Such 2-D ordered structures can find application as antireflective coatings, with a stealth “moth eye” effect.

AUTHOR INFORMATION

Corresponding Author

*E-mail: rabibrata@che.iitkgp.ernet.in (R.M., patterning and AFM); pkbiswas@cgcri.res.in (P.K.B., sol–gel processing). Tel.: +91 3222 283912 (R.M.); +91 33 24833082 (P.K.B.). Fax: +91 3222 255303 (R.M.).

Present Address

[†]Temple University, Philadelphia, PA, USA.

Notes

The authors declare no competing financial interest.

ACKNOWLEDGMENTS

The authors thank the Director, CGCRI, Kolkata, for support and encouragement. This work is funded by DST (Sanction Order No. DST/TSG/PT/2006/74), Government of India. D.S. and R.D.R. acknowledge DST, India, for research fellowships. R.M. acknowledges a DST Fast Track project grant (SR/FTP/ETA-02/06).

REFERENCES

- (1) Madou, M. J. *Fundamentals of Micro Fabrication and Nanotechnology*, 3rd ed.; Taylor and Francis: London, 2011.
- (2) Rondelez, Y.; Tresset, G.; Tabata, K. V.; Arata, H.; Fujita, H.; Takeuchi, S.; Noji, H. Microfabricated arrays of femtoliter chambers allow single molecule enzymology. *Nat. Biotechnol.* **2005**, *23*, 361–365.
- (3) Martines, E.; Seunarine, K.; Morgan, H.; Gadegaard, N.; Wilkinson, C. D. W.; Riehle, M. O. Superhydrophobicity and superhydrophilicity of regular nanopatterns. *Nano Lett.* **2005**, *5*, 2097–2103.
- (4) Sato, O.; Kubo, S.; Gu, Z.-Z. Structural Color Films with Lotus Effects, Superhydrophilicity, and tunable stop-bands. *Acc. Chem. Res.* **2009**, *42*, 1–10.
- (5) Ghatak, A.; Mahadevan, L.; Chung, J. Y.; Chaudhury, M. K.; Shenoy, V. Peeling from a biomimetically patterned thin elastic film. *Proc. R. Soc. London, A* **2004**, *460*, 2725–2735.
- (6) Whitesides, G. M. The Origins and the Future of Microfluidics. *Nature* **2006**, *442*, 368–373.
- (7) Xia, Y.; Whitesides, G. M. Soft Lithography. *Angew. Chem., Int. Ed.* **1998**, *37*, 550–575.
- (8) Gates, B. D.; Xu, Q.; Stewart, M.; Ryan, D.; Willson, C. G.; Whitesides, G. M. New Approaches to Nanofabrication: Molding, Printing, and Other Techniques. *Chem. Rev.* **2005**, *105*, 1171–1196.
- (9) Suh, K. Y.; Kim, Y. S.; Lee, H. H. Capillary Force Lithography. *Adv. Mater.* **2001**, *13*, 1386–1389.
- (10) Yoon, H.; Kim, T.; Choi, S.; Suh, K. Y.; Kim, M. J.; Lee, H. H. Capillary force lithography with impermeable molds. *Appl. Phys. Lett.* **2006**, *88*, 254104 (3 pp).
- (11) Kim, E.; Xia, Y.; Whitesides, G. M. Polymer microstructures formed by moulding in capillaries. *Nature* **1995**, *376*, 581–584.
- (12) Xia, Y.; Kim, E.; Zhao, X. M.; Rogers, J. A.; Prentiss, M.; Whitesides, G. M. Complex optical surfaces formed by replica molding against elastomeric masters. *Science* **1996**, *273*, 347–349.
- (13) Jeon, S.; Menard, E.; Park, J.-U.; Maria, J.; Meitl, M.; Zaumseil, J.; Rogers, J. A. Three-dimensional nanofabrication with rubber stamps and conformable photomasks. *Adv. Mater.* **2004**, *16*, 1369–1373.
- (14) Chou, S. Y.; Krauss, P. R.; Renstrom, P. J. Imprint of sub-25 nm vias and trenches in polymers. *Appl. Phys. Lett.* **1995**, *67*, 3114–3117.
- (15) Chou, S. Y.; Karuss, P. R.; Renstrom, P. J. Imprint Lithography with 25-Nanometer Resolution. *Science* **1996**, *272*, 85–87.
- (16) Benedetto, F. D.; Biasco, A.; Pisignano, D.; Cingolani, R. Patterning polyacrylamide hydrogels by Soft Lithography. *Nanotechnology* **2005**, *16*, 165–170.
- (17) Love, J. C.; Anderson, J. R.; Whitesides, G. M. Fabrication of three dimensional microfluidic system by Soft Lithography. *MRS Bull.* **2001**, *26*, 523–528.
- (18) Kumar, A.; Whitesides, G. M. Features of gold having micrometer to centimeter dimensions can be formed through a combination of stamping with an elastometric stamp and an alkenethiol “ink” followed by chemical etching. *Appl. Phys. Lett.* **1993**, *63*, 2002–2004.
- (19) Gonuguntla, M.; Sharma, A.; Mukherjee, R.; Subramanian, S. A. Control of self-organized contact instability and patterning in soft elastic films. *Langmuir* **2006**, *22*, 7066–7071.
- (20) Mukherjee, R.; Sharma, A. Creating self-organized sub-micron contact instability patterns in soft elastic bilayers with a topographically patterned stamp. *ACS Appl. Mater. Interfaces* **2012**, *4*, 355–363.

- (21) Suh, K. Y.; Lee, H. H. Self organized polymeric microstructures. *Adv. Mater.* **2002**, *14*, 346–351.
- (22) Mukherjee, R.; Sharma, A.; Patil, G.; Faruqui, D.; Pattader, P. S. G. Soft Lithography meets self-organization: Some new developments in meso-patterning. *Bull. Mater. Sci.* **2008**, *31*, 249–261.
- (23) Mukherjee, R.; Patil, G. K.; Sharma, A. Solvent Vapor-Assisted Imprinting of Polymer Films Coated on Curved Surfaces with Flexible PVA Stamps. *Ind. Eng. Chem. Res.* **2009**, *48*, 8812–8818.
- (24) Mukherjee, R.; Sharma, A.; Gonuguntla, M.; Patil, G. K. Adhesive force assisted imprinting of soft solid polymer films by flexible foils. *J. Nanosci. Nanotechnol.* **2008**, *8*, 3406–3415.
- (25) Kim, E.; Xia, Y.; Whitesides, G. M. Micromolding in capillaries: Applications in materials science. *J. Am. Chem. Soc.* **1996**, *118*, 5722–5731.
- (26) Zhao, X. M.; Xia, Y.; Whitesides, G. M. Fabrication of three-dimensional micro-structures: Microtransfer molding. *Adv. Mater.* **1996**, *8*, 837–840.
- (27) Trau, M.; Yao, N.; Kim, E.; Xia, Y.; Whitesides, G. M.; Aksay, I. A. Microscopic patterning of orientated mesoscopic silica through guided growth. *Nature* **1997**, *390*, 674–676.
- (28) Marzolin, C.; Smith, S. P.; Prentiss, M.; Whitesides, G. M. Fabrication of Glass Microstructures by Micro-Molding of Sol-gel Precursors. *Adv. Mater.* **1998**, *10*, 571–574.
- (29) Beh, W. S.; Xia, Y.; Qin, D. Formation of patterned microstructures of polycrystalline ceramics from precursor polymers using micromolding in capillaries. *J. Mater. Res.* **1999**, *14*, 3995–4003.
- (30) Seraji, S.; Wu, Y.; Jewell-Larson, N. E.; Forbess, M. J.; Limmer, S. J.; Chou, T. P.; Cao, G. Patterned Microstructure of Sol-Gel Derived Complex Oxides Using Soft Lithography. *Adv. Mater.* **2000**, *12*, 1421–1424.
- (31) Auger, M. A.; Schilardi, P. L.; Caretti, I.; Sanchez, O.; Benitez, G.; Alabella, J.; Gago, R.; Fonticelli, M.; Vazquez, L.; Salvarezza, R. C.; Azzaroni, O. Molding and Replication of Ceramic Surfaces with Nanoscale Resolution. *Small* **2000**, *1*, 300–309.
- (32) Yang, P. D.; Rizvi, A. H.; Messer, B.; Stucky, B. F.; Whitesides, G. M.; Stucky, G. D. Patterning porous oxides with micro channel networks. *Adv. Mater.* **2001**, *13*, 427–431.
- (33) Heule, M.; Gauckler, L. J. Gas Sensors Fabricated from Ceramic Suspensions by Micromolding in Capillaries. *Adv. Mater.* **2001**, *13*, 1790–1793.
- (34) Yang, H.; Deschatelets, P.; Brittain, S. T.; Whitesides, G. M. Fabrication of High Performance Ceramic Microstructures from a Polymeric Precursor Using Soft Lithography. *Adv. Mater.* **2001**, *13*, 54–58.
- (35) Yu, M.; Lin, J.; Wang, Z.; Fu, J.; Wang, S.; Zhang, H. J.; Han, Y. C. Fabrication, Patterning, and Optical Properties of Nanocrystalline $\text{YVO}_4:\text{A}$ ($\text{A} = \text{Eu}^{3+}, \text{Dy}^{3+}, \text{Sm}^{3+}, \text{Er}^{3+}$) Phosphor Films via Sol-Gel Soft Lithography. *Chem. Mater.* **2002**, *14*, 2224–2231.
- (36) Vartuli, J. S.; Ozenbas, M.; Chun, C. M.; Trau, M.; Aksay, I. A. Micropatterned lead zirconium titanate thin films. *J. Mater. Res.* **2003**, *18*, 1259–1265.
- (37) Martin, C. R.; Aksay, I. A. Topographical evolution of lead zirconate titanate (PZT) thin films patterned by micromolding in capillaries. *J. Phys. Chem. B* **2003**, *107*, 4261–4268.
- (38) Yu, M.; Lin, J.; Fu, J.; Han, Y. C. Sol-gel fabrication, patterning and photoluminescent properties of $\text{LaPO}_4:\text{Ce}^{3+}, \text{Tb}^{3+}$ nanocrystalline thin films. *Chem. Phys. Lett.* **2003**, *371*, 178–183.
- (39) Kim, W. S.; Kim, K. S.; Kim, Y. C.; Bae, B. S. Thermowetting embossing nanoimprinting of the organic-inorganic hybrid materials. *Thin Solid Films* **2005**, *476*, 181–184.
- (40) Yuan, X. C.; Yu, W. X.; He, M.; Bu, J.; Cheong, W. C.; Niu, H. B.; Peng, X. Soft-Lithography-enabled fabrication of large numerical aperture refractive microlens array in hybrid $\text{SiO}_2-\text{TiO}_2$ sol-gel glass. *Appl. Phys. Lett.* **2005**, *86*, 114102 (3 pp).
- (41) Sil, D.; Deb Roy, R.; Jana, S.; Mukherjee, R.; Bhadra, S. K.; Biswas, P. K. Patterning of sol gel thin films by capillary force assisted Soft Lithographic technique. *J. Sol-Gel Sci. Technol.* **2011**, *59*, 117–127.
- (42) Goh, C.; Coakley, K. M.; McGehee, M. D. Nanostructuring Titania by Embossing with Polymer Molds Made from Anodic Alumina Templates. *Nano Lett.* **2005**, *5*, 1545–1549.
- (43) Gobel, O. F.; Nedelcu, M.; Steiner, U. Soft Lithography of Ceramic Patterns. *Adv. Funct. Mater.* **2007**, *17*, 1131–1136.
- (44) Fernández-Sánchez, C.; Cadarso, V. J.; Darder, M.; Domínguez, C.; Llobera, A. Patterning High-Aspect-Ratio Sol-Gel Structures by Microtransfer Molding. *Chem. Mater.* **2008**, *20*, 2662–2668.
- (45) Khan, S. U.; Gobel, O. F.; Blank, D. H. A.; Elshof, J. E. Patterning Lead Zirconate Titanate nanostructures at sub-200-nm resolution by soft confocal imprint lithography and nanotransfer molding. *ACS Appl. Mater. Interface* **2009**, *1*, 2250–2255.
- (46) Peroz, C.; Chauveau, V.; Barthel, E.; Søndergaard, E. Nano-imprint Lithography on Silica Sol-Gels: A Simple Route to Sequential Patterning. *Adv. Mater.* **2009**, *21*, 555–558.
- (47) Roy, S.; Ansari, K. J.; Jampa, S. S. K.; Vutukuri, P.; Mukherjee, R. Influence of Substrate Wettability on the Morphology of Thin Polymer Films Spin-Coated on Topographically Patterned Substrates. *ACS Appl. Mater. Interfaces* **2012**, *4*, 1887–1896.
- (48) Mukherjee, R.; Pangule, R. C.; Sharma, A.; Banerjee, I. Contact instability of thin elastic films on patterned substrates. *J. Chem. Phys.* **2007**, *127*, 064703 (6 pp).
- (49) Biswas, P. K.; Kundu, D.; Ganguli, D. A sol-gel derived antireflective coating on optical glass for near-infrared applications. *J. Mater. Sci. Lett.* **1989**, *8*, 1436–1437.
- (50) Khedkar, S. P.; Radhakrishnan, S. Application of dip-coating process for depositing conducting polypyrrole films. *Thin Solid Films* **1997**, *303*, 167–172.
- (51) Avnir, D. Organic Chemistry within Ceramic Matrixes: Doped Sol-Gel Materials. *Acc. Chem. Res.* **1995**, *28*, 328–334.
- (52) Visovsky, N. J.; Ukrainczyk, L.; Dawes, S. B. Fabrication of micrometer and nanometer scale structures in silica sol-gel films using electron beam writing methods. *J. Vac. Sci. Technol.* **2002**, *20*, 932–935.